HHS Public Access

Author manuscript

Prostate. Author manuscript; available in PMC 2016 May 01.

Published in final edited form as:

Prostate. 2015 May ; 75(6): 593–602. doi:10.1002/pros.22941.

Nanomicellar TGX221 blocks xenograft tumor growth of prostate cancer in nude mice

Ruibao Chen[1,4], **Yunqi Zhao**[2,#], **Yan Huang**[1,#], **Qiuhong Yang**[2], **Xing Zeng**[1,4], **Wencong Jiang**[3], **Jihong Liu**[4], **J. Brantley Thrasher**[1], **M. Laird Forrest**[2], and **Benyi Li**[1,3,*]

[1]Department of Urology, The University of Kansas Medical Center, Kansas City, KS 66160

[2]Department of Pharmaceutical Chemistry, The University of Kansas, Lawrence, KS 66047

[3]Department of Urology, The Affiliated Hospital, Guangdong Medical College, Zhanjiang 524001, China

[4]Department of Urology, Tongji Hospital, Huazhong University of Science & Technology, Wuhan 430030, China

Abstract

Background—Combination of androgen ablation along with early detection and surgery has made prostate cancer highly treatable at the initial stage. However, this cancer remains the second leading cause of cancer death among American men due to castration-resistant progression, suggesting that novel therapeutic agents are urgently needed for this life-threaten condition. Phosphatidylinositol 3-kinase p110β is a major cellular signaling molecule and has been identified as a critical factor in prostate cancer progression. In a recent report, we established a nanomicelle-based strategy to deliver p110β-specific inhibitor TGX221 to prostate cancer cells by conjugating the surface of nanomicelles with a RNA aptamer against prostate membrane specific antigen (PSMA) present in all clinical prostate cancers. In this study, we tested this nanomicellar TGX221 for its *in vivo* anti-tumor effect in mouse xenograft models.

Methods—Prostate cancer cell lines LAPC-4, LNCaP, C4-2 and 22RV1 were used to establish subcutaneous xenograft tumors in nude mice. Paraffin sections from xenograft tumor specimens were used in immunohistochemistry assays to detect AKT phosphorylation, cell proliferation marker Ki67 and PCNA, as well as BrdU incorporation. Quantitative PCR assay was conducted to determine PSA gene expression in xenograft tumors.

Results—Although systemic delivery of unconjugated TGX221 significantly reduced xenograft tumor growth in nude mice compared to solvent control, the nanomicellar TGX221 conjugates completely blocked tumor growth of xenografts derived from multiple prostate cancer cell lines. Further analyses revealed that AKT phosphorylation and cell proliferation indexes were dramatically reduced in xenograft tumors received nanomicellar TGX221 compared to xenograft

[*]Corresponding author: Benyi Li, MD/PhD, KUMC Urology, 3901 Rainbow Blvd, MS 3035, Kansas City, KS 66160. bli@kumc.edu. Tel: 913.588.4773.

[#]Current address: Yan Huang, MD/PhD, Department of Ultrasound Imaging, Nanjing First Hospital, Nanjing Medical University, Nanjing 210029, China; Yunqi Zhao, PhD, School of Pharmacy, Kunming Medical University, Kunming 650500, China

tumors received unconjugated TGX221 treatment. There was no noticeable side effect by gross observation or at microscopic level of organ tissue section.

Conclusion—These data strongly suggest that prostate cancer cell-targeted nanomicellar TGX221 is an effective anti-cancer agent for prostate cancer.

Keywords

prostate cancer; p110β; nanotechnology; micelle; TGX221; cancer therapy

Introduction

The development of nano-scaled drug carriers is a prominent area of anti-cancer therapeutic development because these nano-scaled carriers can be easily modified to achieve tissue-specific drug delivery and improved pharmacokinetics (1,2). Currently, various types of materials have been used to fabricate nano-scaled drug carriers, including polymeric, inorganic (e.g. quantum dots, carbon nanotubes, and gold nanoparticles) and nuclear acid (RNA and DNA molecules) materials (2-4). So far US FDA has approved several nanomedicines for clinical use (2).

Self-assembled core-shell nanocarriers (i.e. micelles) are capable of solubilizing a wide range of hydrophobic molecules (5) and are a potential tool for the safe formulation and delivery of antitumor agents to tumors without the inclusion of potentially harmful surfactants and excipients such as DMSO and propylene glycol (6). Due to their nanoscopic dimensions (< 100 nm), micelles can leave leaky vasculature, accumulating in tumors via the enhanced permeability and retention effect (EPR), where they remain due to poor lymphatic clearance. An outer coat of poly(ethylene glycol) (PEG) imparts “stealth” characteristics to micelles, allowing them to circulate for long periods of time and avoid accumulation in reticular endothelial system (RES) of the liver and spleen, as demonstrated in our previous reports (7-9). These effects potentially reduce non-specific toxicities by improving the drug's efficacy and enlarging the therapeutic window.

Phosphatidylinositol 3-kinases (PI3K) are a family of intracellular signaling molecules that regulate multiple signal pathways (10). There are three classes (I, II and III) of PI3K isoforms in mammalian cells, of which the class I PI3Ks p110α and p110β are ubiquitously expressed, and knocking out either one of these two genes in mice resulted in embryonic lethal (11). Recently, we discovered that p110β is expressed at a significantly higher level in prostate cancer tissues and cell lines compared to p110α and that p110β but not p110α is critical in androgen-stimulated cell proliferation, AR-mediated gene expression and xenograft tumor growth of xenografts derived from AR-positive prostate cancer cells in nude mice (12). We also determined that p110β expression is largely elevated in malignant prostate tissues compared to their surrounding non-malignant counterparts and its mRNA levels correlate with disease progression in prostate cancer patients (12). Our findings were supported by other groups using transgenic mouse models (13,14) and cell culture models (15). Taken together, these data indicate that targeting p110beta represents a potential therapeutic approach prostate cancer management.

TGX-221 is a synthetic small molecule inhibitor and displays a wonderful isoform-specificity towards p110β over other type IA PI3Ks (16). It has been successfully used in animal models to suppress p110β activity *in vivo* (17). However, TGX-221 is very poorly water soluble, requiring organic solvents such as DMSO and propylene glycol for intravenous injection, which have significant cardiac toxicity and may cause unconsciousness, arrhythmia, and cardiac arrest (18). Therefore, a cancer cell-targeted and water soluble formulation of this compound for human use is highly desirable. For this purpose, we recently synthesized a TGX221 analog BL05 that was encapsulated in a polymeric micelle (19). The surface of TGX221-BL05-loaded micelle was conjugated with a RNA aptamer against prostate membrane specific antigen (PSMA) present in all clinical prostate cancers (20). Our initial *in vitro* experiments demonstrated that PSMA aptamer-conjugated nanomicellar TGX221 formulation has a 2.27-fold greater in the plasma concentration and a 6.16-fold slower in drug clearance rate than that of the naked drug in nude mice, suggesting a potential prostate cancer-targeted treatment. In this study, we evaluated the *in vivo* anti-tumor activity of the nanomicellar TGX221 formula in mouse xenograft tumor model of prostate cancer. Our data revealed that nanomicellar TGX221 completely blocked xenograft tumor growth in nude mice derived from multiple prostate cancer cell lines. This drastic anti-tumor effect was associated with significant inhibition of AKT phosphorylation and cell proliferation in xenograft tumors.

Materials and Methods

Cell Culture, Antibodies and Reagents

Human prostate cancer LNCaP and 22RV1 cells were obtained from the American Type Culture Collection (Manassas, VA). C4-2 cell line was obtained from UroCor Inc (Oklahoma City, OK). LAPC-4 cells were from Dr. Charles L. Sawyers (21) and maintained in Iscoves medium with 15% FBS/1% L-glutamine and antibiotics. Other cell lines were maintained in RPMI 1640 supplemented with 10% fetal bovine serum (FBS) plus antibiotics (Invitrogen, Carlsbad, CA). Antibodies for phospho-AKT serine 473 (sc-101629), Ki67 (clone H-300, sc-15402) and proliferating cell nuclear antigen (PCNA, clone PC10, sc-56) were purchased from Santa Cruz Biotech (Santa Cruz, CA).

Animal Experiments, BrdU Labeling Assay and Immunohistochemistry

All animal studies were conducted under an approved Institutional Animal Care and Use Committee protocol. To determine the maximum tolerable dose (MTD) in animals, 5 group of nude mice (n = 3) were received intravenous (*i.v.*) injection of either BL05 dissolved in polypropylene glycol (PPG) or A10-conjugated BL05 loaded nano-micelles at 5 different doses (6.25, 12.5, 25, 50 and 100 mg/kg body weight). One additional group of animals were received the solvent PPG as control. Animals were monitored for 5 days for any sign of toxicity. No obvious evidence of side effects, including loss of appetite, loss of weight, reduced movement, sickness or death, was noticed. At necropsy, no macroscopic or microscopic sign or evidence for tissue/organ damage/bleeding or necrosis was observed in major organs, such as liver, spleen, lung, kidney, prostate, testis etc.

For xenograft experiments in nude mice, we used four prostate cancer cell lines, androgen-responsive LAPC-4 & LNCaP and castration-resistant C4-2 & 22RV1 to generate the subcutaneous xenografts. Cell suspension (2×10^6 cells in 0.1 ml of serum-free culture media) were inoculated subcutaneously (*s.c.*) into the rear flanks (2 sites/mouse) of 6-weeks-old male nude mice (Charles River, Wilmington, MA). Once xenograft tumors were palpable (about 30 mm^3 in size), animals were randomly divided into three groups (n = 8) and were treated with the solvent PPG (as the solvent control group), naked TGX221 pro-drug BL05 in PPG (naked TGX221 group) and PSMA A10 aptamer-conjugated nanocarrier with BL05 (Nano-TGX221 group). The total volume of drug solution was 200 μl for tail vein injection twice a week and the TGX221 was used at a dose of 100 mg/kg bodyweight.

Tumor growth was monitored twice a week with a caliper. Tumor volume was calculated by the formula of $L \times W \times H \times 0.5236$ (22) and tumor growth curve was generated by plotting the relative fold value of tumor volume at each time points comparing to their initial volume (set to value 1). The formula of calculation was $([V_{tp} - V_0]/V_0) \times 100\%$; V_{tp} indicates tumor volume at each time-points; V_0 indicates the initial volume at day 0 of treatment. In control group when the volume of xenograft tumors reached the limit of tumor burden set by our IACUC, animals were sacrificed and xenograft tumors were dissected. After tumor dissection, half of the tumor specimens were stored in -80C for further analysis and another half of the specimens were subjected for paraffin embedding process.

5-bromo-2-deoxyuridine (BrdU) labeling assay was conducted to label the newly synthesized DNA for evaluating tumor cell proliferation. At the end of experiments one hour before sacrifice, the animals were injected intraperitoneally (*i.p.*) with 0.5 ml of a 10-mM BrdU solution one hour before necropsy/sacrifice. To detect BrdU labeled cells in tissues, paraffin-embedded tissue sections were immunostained for incorporated BrdU using ZYMED BrdU Staining Kit (Invitrogen).

To detect apoptotic cell death in xenograft tumors, terminal deocynucleotide transferase dUTP nick end labeling (TUNEL) assay was conducted using Apo-BrdU-IHCTM *in situ* DNA Fragmentation Assay Kit (BioVision, Mountain View, CA), as described in our previous publication (23).

Immunostaining for anti-pAKT (S473), anti-Ki67 and anti-PCNA was conducted as described in our previous publication (23). Briefly, paraffin-embedded tissue sections were de-paraffinized and re-hydrated. Antigen recovery was achieved by boiling the sections in citrate acid buffer (10 mM, pH 6.0). The sections were incubated with the primary antibodies overnight at 4C and visualized using a DAKO LSAB+ Detection System (catalog #K0679, DAKO USA). The immunostaining results were expressed as a semi-quantitative index as described in our previous publication (24). Briefly, the intensity of the immunosignals was scored as 0 (negative), 1 (weak), 2 (moderate), and 3 (strong). The immunosignal index was calculated by multiplying the average intensity score with the percentage of positive cancer cells from at least 5 microscopic fields.

Tissue distribution of TGX221-loaded PSMA A10-nanomicelles was assessed by administering the formula at doses of 100, 50, 25, 12.5 and 6.25 mg/kg bodyweight in nude

mice bearing subcutaneous LNCaP xenografts (n = 3). Major organs (kidney, intestine, prostate, liver and spleen) and xenografts were excised after 5 days. For each tissue specimens, 15 mg of sample was digested with proteinase K, and the amount of TGX221 was determined (μg/mg tissue) by HPLC as described in our initial publication (19).

RNA Extraction and Real-Time Reverse Transcription (RT)-PCR

Total tissue RNAs were prepared using Tri-Reagent (Invitrogen). To assess mRNA expression, a quantitative reverse transcription-PCR (qRT-PCR) assay was conducted using the SYBR Green-based approach on the Bio-Rad iQ5 system. The primer pairs for human *PSA* gene (forward 5′-ACCAGAGGAGTTCTTGACC CCAAA-3′; backward 5′-CCCCAGAATCA CCCGAGCAG-3′) were described in our previous publication (25). Human *KRT18* gene (forward 5′-CCAGTCTGTGGAGAACGACA-3′; backward 5′-CTGGGCTTGTAGGCCTTTT AC-3′) was used as the internal control. The primers were synthesized by IDT (Coralville, IA). The qPCR counts were normalized against the value for the epithelial cell-specific gene *KRT18* as described in our previous publication (25).

Statistical Analysis

Microscopic images of immunostaining results are presented from representative experiments. The mean and the standard error of the mean (SEM) were shown for tumor growth, BrdU labeling, TUNEL index, pAKT, Ki67, and PCNA immunostaining signal index, as well as qPCR data. The significance of differences between groups were analyzed by ANOVA analysis as described in our previous publications (12,23,25) using the SPSS computer software (SPSS, Inc., Chicago, IL).

Results

Nanomicellar TGX221 is mainly distributed within prostate cancer xenografts

In the initial phase of this project, we synthesized a TGX221 analog BL05 with a fatty acid modification (Fig 1A) so that the drug could be encapsulated into polymeric nanomicelle. The surface of the nanomicelle was conjugated with a RNA aptamer PSMA A10 to achieve prostate cancer-targeted delivery (26). The whole process of chemical synthesis and nanomicelle fabrication were described in our recent report (19). Then, the maximum tolerable dose and tissue distribution profile were determined in nude mice bearing xenograft tumors derived from prostate cancer LNCaP cell line. At the maximum dose of 100 mg/kg bodyweight that was tested, no noticeable toxicity was observed at either gross observation or microscopic analysis of major organs (Fig 1B). Therefore, the dose of 100 mg/kg bodyweight was used for the subsequent experiments. Tissue distribution assay revealed that after injection of naked or nanomicellar TGX221 (analog BL05), much higher levels of TGX221 (analog BL05) were detected in xenograft tumors, intestine, liver and prostate tissues than that in other organs (Fig 1C). The order of relative concentration of TGX221 in animals was as follow: xenograft > intestine > liver > prostate > spleen > kidney. This profile of tissue distribution suggested that the nanomicellar TGX221 formulation is suitable for systemic delivery as an anti-cancer agent.

Nanomicellar TGX221 completely blocks xenograft tumor growth in nude mice

Then, we tested the anti-tumor effect of the nanomicellar TGX221 formulation in mouse xenograft models. Four prostate cancer cell lines, androgen-responsive LAPC-4 and LNCaP as well as castration-resistant C4-2 and 22RV1, were used to establish *s.c.* xenograft tumors in nude mice. As shown in Fig 2, compared to the solvent control, treatment with nanomicellar TGX221 completely blocked xenograft tumor growth derived from all four cell lines. In contrast, treatment of animals with naked TGX221 without nanomicelle formulation only blocked tumor growth of xenografts derived from LAPC-4 and C4-2 cells (Fig 2A&2D) but not from LNCaP and 22RV1 cells although naked TGX221 suppressed xenograft tumor growth by 40-60% compared to the solvent control in these two xenograft models (Fig 2B&2C). These data indicated that nanomicellar TGX221 has a significant advantage over naked drug in blocking tumor growth of prostate cancers.

Nanomicellar TGX221 completely abolishes AKT phosphorylation and cell proliferation in xenograft tumor

After treatment, xenograft tumor specimens were dissected for immunohistochemical analysis of PI3K downstream protein AKT phosphorylation and cell proliferation index. As shown in Fig 3A, immunosignals for AKT phosphorylation were very strong in xenograft tumors from the control group. Treatment with naked TGX221 largely reduced the immunosignals of phosphor-AKT. These immunosignals were almost abolished in nanomicellar TGX221-treated xenograft tumors. Quantitative data were summarized in Fig 3E.

Similarly, tumor cell proliferation indexes were assessed by detecting Ki67 and PCNA immunosignals as well as BrdU labeling in xenograft tissues. As shown in Fig 3B-3C, 3F-3G and Fig 4A, these cell proliferation indexes were dramatically reduced in nanomicellar TGX221-treated xenograft tumors compared to the solvent control although naked TGX221-treated tumors also showed a significant lower index than that in the control group. These data are consistent with the tumor growth curve as measured by tumor size (Fig 2), indicating that nanomicellar TGX221 has a strong inhibitory effect *in vivo* on tumor cell proliferation by suppressing PI3K p110β-AKT signaling in prostate cancer.

Nanomicellar TGX221 induces apoptosis and reduces PSA gene expression in xenograft tumor

Next, we conducted a TUNEL assay to assess if nanomicellar TGX221 treatment induced apoptotic cell death in xenograft tumors. As shown in Fig 3D, clear positive immunosignals were visible on xenograft tumor sections treatment by nanomicellar TGX221 but it was less in naked TGX221-treated xenograft tumors. Quantitative analysis revealed a moderate apoptosis rate in nanomicellar TGX221-treated xenograft tumors but at a very low level in naked TGX221-treated tumor specimens (Fig 3H). These data indicate that apoptosis is not a major event in nanomicellar TGX221-induced suppression of xenograft tumor growth.

Lastly, we analyzed the prostate cancer specific gene *PSA* expression in xenograft tumor tissues by quantitative RT-PCR assays. As shown in Fig 4B, *PSA* gene expression at the mRNA level was significantly reduced in nanomicellar TGX221 treatment group as

compared to the naked drug or the solvent control groups. These data are consistent with our previous reports (12,23,27,28) that PI3K p110β activity is involved in androgen-stimulated gene expression.

Discussion

The goal of this study was to test the *in vivo* anti-tumor effect of nanomicellar TGX221 formulation, a prostate cancer-targeted micelle loaded with the PI3K p110β-specific inhibitor TGX221. Tissue-specific targeting was achieved by conjugating micelle surface with a PSMA-binding RNA aptamer A10, as described in previous reports (19,29). We used four prostate cancer cell lines to establish *s. c*. xenograft models in nude mice for the *in vivo* testing. Animal treatment with the nanomicellar TGX221 did not show a noticeable toxicity even at a much higher dose level of 100 mg/kg body weight. Treatment with the nanomicellar TGX221 completely blocked xenograft tumor growth, which was largely effective than the naked drug solution. These anti-tumor effects were associated with reduced cell proliferation and AKT phosphorylation. Treatment with nanomicellar TGX221 formulation also induced apoptotic cell death and reduced *PSA* gene expression.

Cellular PI3K family consists of multiple isoforms with diverse functions. It is predictable that non-specific inhibition of this major kinase family will result in multiple side effects when it is used in patients (30-32). Currently, multiple PI3K inhibitors are being tested in clinical trials for various human malignancies (33), of which two p110β-specific inhibitors GSK2636771 and SAR260301 are currently in phase I trials on solid tumors including prostate cancer. These two compounds have a slight similarity with TGX221 in molecular structure but SAR260301 has more drug-like properties including high water solubility and oral bioavailability (34). However, by taking the advantage of nanotechnology, nanomicelle conjugation of TGX221 greatly enhanced drug plasma concentration (19) and prostate cancer tumor tissue distribution in mice (Fig 1C). Although bleeding issues might be a clinical concern due to the critical role of p110β in blood platelet function (35), no obvious bleeding lesion was noticed grossly or microscopically on tissue sections from major organs of mice even after treatment with a MTD dose. These results indicate that prostate cancer cell-specific delivery of TGX221 with PSMA aptamer conjugation devoid of other cardiovascular actions.

As a unique cell surface protein, PSMA has been widely used as a biomarker in prostate cancer-targeted therapy and imaging (36). For example, we have successfully delivered PSMA-targeting RNA aptamer-conjugated poly(lactic-co-glycolic acid) (PLGA) nanoparticles to prostate cancer cells in a tissue-specific fashion (37). Similarly, in this study, the highest level of nanomicellar TGX221 accumulation was detected in prostate cancer tissues. Meanwhile, we also noticed that intestine and liver tissues had a relatively higher level of the drug (Fig 1C), which is consistent with previous reported that PSMA is also expressed in small intestine and liver tissues (38,39).

Recently, personalizing prostate cancer therapy has been emerging as a new trend of patient care due to heterogeneity of the disease (40,41). Alterations of PI3K-AKT-PTEN axis were reported in about 40-70% of primary and metastatic prostate cancers (41,42) and p110β has

been shown as a predominant factor for prostate cancer progression (12-15), therefore, the nanomicellar TGX221 might be used as a personalized therapy for p110β overactive patients due to gene overexpression or *PTEN*-loss mutation. However, a reciprocal feedback regulation of PI3K pathway and the AR signaling was determined in prostate cancer animal models (43); the nanomicellar TGX221 formulation might be used together with an effective anti-AR therapy like Enzalutamide to overcome any potential resistance.

In conclusion, we demonstrated that nanomicellar TGX221 was effective in blocking tumor growth of prostate cancer xenografts in nude mice. This anti-tumor effect was associated with reduced AKT phosphorylation and tumor cell proliferation. Our data suggest that the nanomicellar TGX221 formulation might be used as one component of personalized medicine for prostate cancer patients who are harboring alterations in PI3K pathway.

Acknowledgments

The project was supported by DoD PCRP Grant (W81XWH-09-1-0455) to Drs Benyi Li and Laird Forrest. It is also partially supported by grants from NCI#1R21CA175279-01A1 and Chinese NSF Grant (CNSF#81172427) to Dr Benyi Li, as well as the grant of NCI R01CA173292 to Dr Laird Forrest. The research activities in Dr Benyi Li's lab are supported by KU William L. Valk Foundation and KUMC Mason's Foundation.

References

1. Kapse-Mistry S, Govender T, Srivastava R, Yergeri M. Nanodrug delivery in reversing multidrug resistance in cancer cells. Frontiers in pharmacology. 2014; 5:159. [PubMed: 25071577]
2. Dawidczyk CM, Kim C, Park JH, Russell LM, Lee KH, Pomper MG, Searson PC. State-of-the-art in design rules for drug delivery platforms: lessons learned from FDA-approved nanomedicines. Journal of controlled release : official journal of the Controlled Release Society. 2014; 187:133–144. [PubMed: 24874289]
3. Khisamutdinov EF, Jasinski DL, Guo P. RNA as a boiling-resistant anionic polymer material to build robust structures with defined shape and stoichiometry. ACS nano. 2014; 8(5):4771–4781. [PubMed: 24694194]
4. Liu Y, Solomon M, Achilefu S. Perspectives and potential applications of nanomedicine in breast and prostate cancer. Medicinal research reviews. 2013; 33(1):3–32. [PubMed: 23239045]
5. Jhaveri AM, Torchilin VP. Multifunctional polymeric micelles for delivery of drugs and siRNA. Frontiers in pharmacology. 2014; 5:77. [PubMed: 24795633]
6. Xiong MP, Yanez JA, Remsberg CM, Ohgami Y, Kwon GS, Davies NM, Forrest ML. Formulation of a geldanamycin prodrug in mPEG-b-PCL micelles greatly enhances tolerability and pharmacokinetics in rats. Journal of controlled release : official journal of the Controlled Release Society. 2008; 129(1):33–40. [PubMed: 18456363]
7. Forrest ML, Zhao A, Won CY, Malick AW, Kwon GS. Lipophilic prodrugs of Hsp90 inhibitor geldanamycin for nanoencapsulation in poly(ethylene glycol)-b-poly(epsilon-caprolactone) micelles. Journal of controlled release : official journal of the Controlled Release Society. 2006; 116(2):139–149. [PubMed: 16926059]
8. Forrest ML, Won CY, Malick AW, Kwon GS. In vitro release of the mTOR inhibitor rapamycin from poly(ethylene glycol)-b-poly(epsilon-caprolactone) micelles. Journal of controlled release : official journal of the Controlled Release Society. 2006; 110(2):370–377. [PubMed: 16298448]
9. Yanez JA, Forrest ML, Ohgami Y, Kwon GS, Davies NM. Pharmacometrics and delivery of novel nanoformulated PEG-b-poly(epsilon-caprolactone) micelles of rapamycin. Cancer chemotherapy and pharmacology. 2008; 61(1):133–144. [PubMed: 17393166]
10. Klempner SJ, Myers AP, Cantley LC. What a tangled web we weave: emerging resistance mechanisms to inhibition of the phosphoinositide 3-kinase pathway. Cancer discovery. 2013; 3(12):1345–1354. [PubMed: 24265156]

11. Martini M, De Santis MC, Braccini L, Gulluni F, Hirsch E. PI3K/AKT signaling pathway and cancer: an updated review. Annals of medicine. 2014:1–12.
12. Zhu Q, Youn H, Tang J, Tawfik O, Dennis K, Terranova PF, Du J, Raynal P, Thrasher JB, Li B. Phosphoinositide 3-OH kinase p85alpha and p110beta are essential for androgen receptor transactivation and tumor progression in prostate cancers. Oncogene. 2008; 27(33):4569–4579. [PubMed: 18372911]
13. Lee SH, Poulogiannis G, Pyne S, Jia S, Zou L, Signoretti S, Loda M, Cantley LC, Roberts TM. A constitutively activated form of the p110beta isoform of PI3-kinase induces prostatic intraepithelial neoplasia in mice. Proceedings of the National Academy of Sciences of the United States of America. 2010; 107(24):11002–11007. [PubMed: 20534477]
14. Jia S, Liu Z, Zhang S, Liu P, Zhang L, Lee SH, Zhang J, Signoretti S, Loda M, Roberts TM, Zhao JJ. Essential roles of PI(3)K-p110beta in cell growth, metabolism and tumorigenesis. Nature. 2008; 454(7205):776–779. [PubMed: 18594509]
15. Jiang X, Chen S, Asara JM, Balk SP. Phosphoinositide 3-kinase pathway activation in phosphate and tensin homolog (PTEN)-deficient prostate cancer cells is independent of receptor tyrosine kinases and mediated by the p110beta and p110delta catalytic subunits. The Journal of biological chemistry. 2010; 285(20):14980–14989. [PubMed: 20231295]
16. Jackson SP, Schoenwaelder SM, Goncalves I, Nesbitt WS, Yap CL, Wright CE, Kenche V, Anderson KE, Dopheide SM, Yuan Y, Sturgeon SA, Prabaharan H, Thompson PE, Smith GD, Shepherd PR, Daniele N, Kulkarni S, Abbott B, Saylik D, Jones C, Lu L, Giuliano S, Hughan SC, Angus JA, Robertson AD, Salem HH. PI 3-kinase p110beta: a new target for antithrombotic therapy. Nature medicine. 2005; 11(5):507–514.
17. Sturgeon SA, Jones C, Angus JA, Wright CE. Advantages of a selective beta-isoform phosphoinositide 3-kinase antagonist, an anti-thrombotic agent devoid of other cardiovascular actions in the rat. European journal of pharmacology. 2008; 587(1-3):209–215. [PubMed: 18455722]
18. Santos NC, Figueira-Coelho J, Martins-Silva J, Saldanha C. Multidisciplinary utilization of dimethyl sulfoxide: pharmacological, cellular, and molecular aspects. Biochemical pharmacology. 2003; 65(7):1035–1041. [PubMed: 12663039]
19. Zhao Y, Duan S, Zeng X, Liu C, Davies NM, Li B, Forrest ML. Prodrug strategy for PSMA-targeted delivery of TGX-221 to prostate cancer cells. Molecular pharmaceutics. 2012; 9(6):1705–1716. [PubMed: 22494444]
20. Silver DA, Pellicer I, Fair WR, Heston WD, Cordon-Cardo C. Prostate-specific membrane antigen expression in normal and malignant human tissues. Clinical cancer research : an official journal of the American Association for Cancer Research. 1997; 3(1):81–85. [PubMed: 9815541]
21. Klein KA, Reiter RE, Redula J, Moradi H, Zhu XL, Brothman AR, Lamb DJ, Marcelli M, Belldegrun A, Witte ON, Sawyers CL. Progression of metastatic human prostate cancer to androgen independence in immunodeficient SCID mice. Nature medicine. 1997; 3(4):402–408.
22. Plotkin B, Kaidanovich O, Talior I, Eldar-Finkelman H. Insulin mimetic action of synthetic phosphorylated peptide inhibitors of glycogen synthase kinase-3. The Journal of pharmacology and experimental therapeutics. 2003; 305(3):974–980. [PubMed: 12626660]
23. Li B, Sun A, Youn H, Hong Y, Terranova PF, Thrasher JB, Xu P, Spencer D. Conditional Akt activation promotes androgen-independent progression of prostate cancer. Carcinogenesis. 2007; 28(3):572–583. [PubMed: 17032658]
24. Sun A, Tawfik O, Gayed B, Thrasher JB, Hoestje S, Li C, Li B. Aberrant expression of SWI/SNF catalytic subunits BRG1/BRM is associated with tumor development and increased invasiveness in prostate cancers. The Prostate. 2007; 67(2):203–213. [PubMed: 17075831]
25. Chen R, Zeng X, Zhang R, Huang J, Kuang X, Yang J, Liu J, Tawfik O, Thrasher JB, Li B. Cav1.3 channel alpha1D protein is overexpressed and modulates androgen receptor transactivation in prostate cancers. Urologic oncology. 2014; 32(5):524–536. [PubMed: 24054868]
26. Farokhzad OC, Cheng J, Teply BA, Sherifi I, Jon S, Kantoff PW, Richie JP, Langer R. Targeted nanoparticle-aptamer bioconjugates for cancer chemotherapy in vivo. Proceedings of the National Academy of Sciences of the United States of America. 2006; 103(16):6315–6320. [PubMed: 16606824]

27. Liao X, Thrasher JB, Holzbeierlein J, Stanley S, Li B. Glycogen synthase kinase-3beta activity is required for androgen-stimulated gene expression in prostate cancer. Endocrinology. 2004; 145(6): 2941–2949. [PubMed: 14988390]

28. Liu J, Youn H, Yang J, Du N, Liu J, Liu H, Li B. G-protein alpha-s and -12 subunits are involved in androgen-stimulated PI3K activation and androgen receptor transactivation in prostate cancer cells. The Prostate. 2011; 71(12):1276–1286. [PubMed: 21308712]

29. Lupold SE, Hicke BJ, Lin Y, Coffey DS. Identification and characterization of nuclease-stabilized RNA molecules that bind human prostate cancer cells via the prostate-specific membrane antigen. Cancer research. 2002; 62(14):4029–4033. [PubMed: 12124337]

30. Bendell JC, Rodon J, Burris HA, de Jonge M, Verweij J, Birle D, Demanse D, De Buck SS, Ru QC, Peters M, Goldbrunner M, Baselga J. Phase I, dose-escalation study of BKM120, an oral pan-Class I PI3K inhibitor, in patients with advanced solid tumors. Journal of clinical oncology : official journal of the American Society of Clinical Oncology. 2012; 30(3):282–290. [PubMed: 22162589]

31. Rodon J, Brana I, Siu LL, De Jonge MJ, Homji N, Mills D, Di Tomaso E, Sarr C, Trandafir L, Massacesi C, Eskens F, Bendell JC. Phase I dose-escalation and -expansion study of buparlisib (BKM120), an oral pan-Class I PI3K inhibitor, in patients with advanced solid tumors. Investigational new drugs. 2014; 32(4):670–681. [PubMed: 24652201]

32. Shapiro GI, Rodon J, Bedell C, Kwak EL, Baselga J, Brana I, Pandya SS, Scheffold C, Laird AD, Nguyen LT, Xu Y, Egile C, Edelman G. Phase I safety, pharmacokinetic, and pharmacodynamic study of SAR245408 (XL147), an oral pan-class I PI3K inhibitor, in patients with advanced solid tumors. Clinical cancer research : an official journal of the American Association for Cancer Research. 2014; 20(1):233–245. [PubMed: 24166903]

33. Dienstmann R, Rodon J, Serra V, Tabernero J. Picking the point of inhibition: a comparative review of PI3K/AKT/mTOR pathway inhibitors. Molecular cancer therapeutics. 2014; 13(5): 1021–1031. [PubMed: 24748656]

34. Certal V, Carry JC, Halley F, Virone-Oddos A, Thompson F, Filoche-Romme B, El-Ahmad Y, Karlsson A, Charrier V, Delorme C, Rak A, Abecassis PY, Amara C, Vincent L, Bonnevaux H, Nicolas JP, Mathieu M, Bertrand T, Marquette JP, Michot N, Benard T, Perrin MA, Lemaitre O, Guerif S, Perron S, Monget S, Gruss-Leleu F, Doerflinger G, Guizani H, Brollo M, Delbarre L, Bertin L, Richepin P, Loyau V, Garcia-Echeverria C, Lengauer C, Schio L. Discovery and optimization of pyrimidone indoline amide PI3Kbeta inhibitors for the treatment of phosphatase and tensin homologue (PTEN)-deficient cancers. Journal of medicinal chemistry. 2014; 57(3): 903–920. [PubMed: 24387221]

35. Bird JE, Smith PL, Bostwick JS, Shipkova P, Schumacher WA. Bleeding response induced by anti-thrombotic doses of a phosphoinositide 3-kinase (PI3K)-beta inhibitor in mice. Thrombosis research. 2011; 127(6):560–564. [PubMed: 21396684]

36. Ristau BT, O'Keefe DS, Bacich DJ. The prostate-specific membrane antigen: lessons and current clinical implications from 20 years of research. Urologic oncology. 2014; 32(3):272–279. [PubMed: 24321253]

37. Yang J, Xie SX, Huang Y, Ling M, Liu J, Ran Y, Wang Y, Thrasher JB, Berkland C, Li B. Prostate-targeted biodegradable nanoparticles loaded with androgen receptor silencing constructs eradicate xenograft tumors in mice. Nanomedicine. 2012; 7(9):1297–1309. [PubMed: 22583574]

38. Troyer JK, Beckett ML, Wright GL Jr. Detection and characterization of the prostate-specific membrane antigen (PSMA) in tissue extracts and body fluids. International journal of cancer Journal international du cancer. 1995; 62(5):552–558. [PubMed: 7665226]

39. Kinoshita Y, Kuratsukuri K, Landas S, Imaida K, Rovito PM Jr, Wang CY, Haas GP. Expression of prostate-specific membrane antigen in normal and malignant human tissues. World journal of surgery. 2006; 30(4):628–636. [PubMed: 16555021]

40. Cetnar JP, Beer TM. Personalizing prostate cancer therapy: the way forward. Drug discovery today. 2014

41. Fraser M, Berlin A, Bristow RG, van der Kwast T. Genomic, pathological, and clinical heterogeneity as drivers of personalized medicine in prostate cancer. Urologic oncology. 2014

42. Bitting RL, Armstrong AJ. Targeting the PI3K/Akt/mTOR pathway in castration-resistant prostate cancer. Endocrine-related cancer. 2013; 20(3):R83–99. [PubMed: 23456430]

43. Carver BS, Chapinski C, Wongvipat J, Hieronymus H, Chen Y, Chandarlapaty S, Arora VK, Le C, Koutcher J, Scher H, Scardino PT, Rosen N, Sawyers CL. Reciprocal feedback regulation of PI3K and androgen receptor signaling in PTEN-deficient prostate cancer. Cancer cell. 2011; 19(5):575–586. [PubMed: 21575859]

Abbreviation

AR	androgen receptor
BrdU	5-bromo-2-deoxyuridine
EPR	enhanced permeability and retention
FBS	fetal bovine serum
FDA	federal drug&food administration
MTD	maximum tolerable dose
Nano	nanometer
PCNA	proliferating cell nuclear antigen
PEG	polypropylene glycol
PI3K	phosphatidylinositol 3-kinases
PLGA	poly(lactic-co-glycolic acid)
PPG	poly(ethylene glycol)
PSA	prostate specific antigen
PSMA	prostate membrane specific antigen
RES	reticular endothelial system
SEM	standard error of the MEAN
TUNEL	terminal deocynucleotide transferase dUTP nick end labeling
US FDA	United States Food and Drug Administration

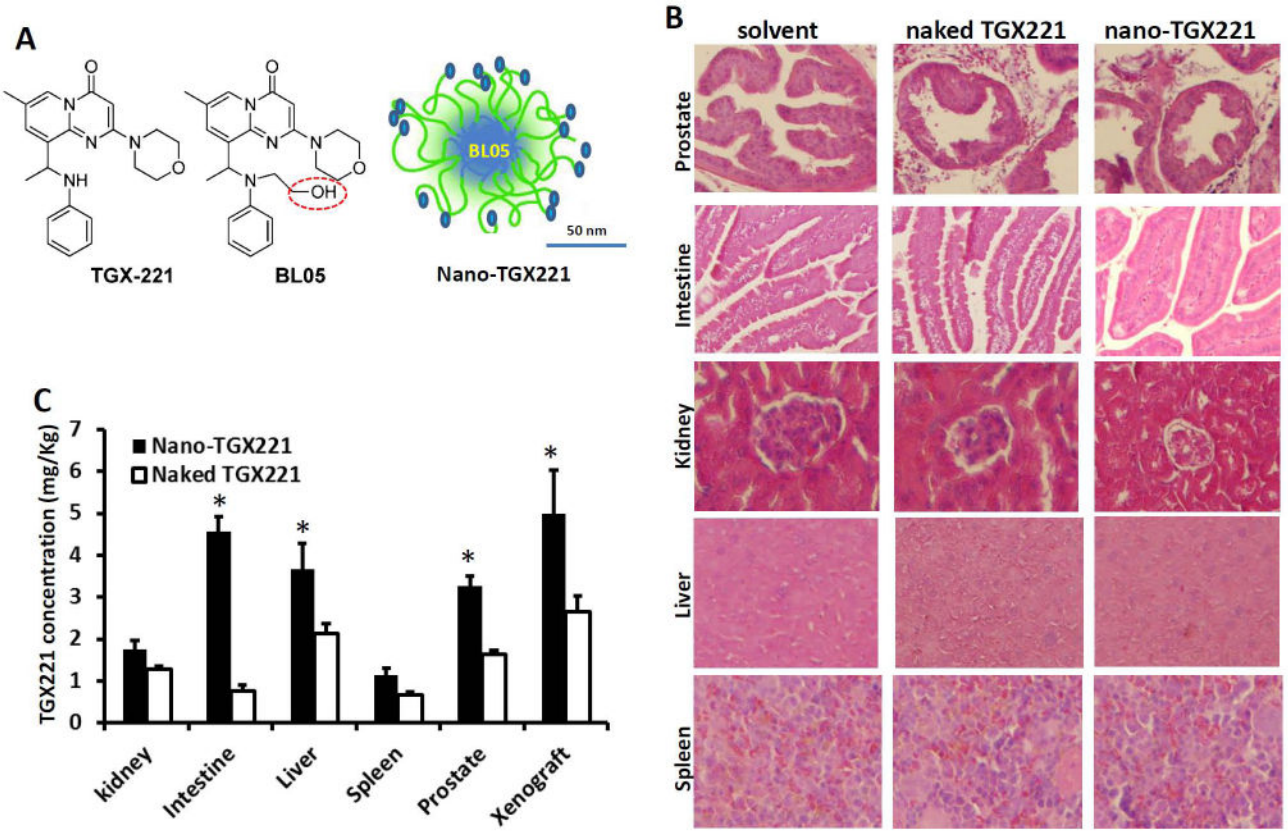

Fig 1.

A Scheme of the molecular structure of TGX221 and its analog BL05, as well as nanomicellar TGX221-BL05 formulation. Circled in red line indicates the modified position on TGX221 for conjugation with micelle polymers. Scale bar, 50 nm.

B Microscopic images of mice organs. Mice were treated with the solvent (PPG, 200 μl), TGX221-BL05 in polypropylene glycol (PPG) solution (naked TGX221) and nanomicellar TGX221 formulation (nano-TGX221). Drugs were injected via tail vein at a dose of 100 mg/kg bodyweight in 200 μl PPG solution. Animals were sacrificed at day 5 after drug delivery and the major organs as indicated on the left side of the panels were dissected for histological analysis after H&E staining. Magnification, × 200.

C. Tissue distribution of the delivered drug TGX221. Mice tissues harvested at autopsy described in panel B were homogenized for quantitative measurement of the TGX221 compound. Data were presented as Mean (n = 3) and error bars indicate the SEM. The asterisk indicates significant difference compared to the naked drug ($P < 0.05$, Student *t*-test).

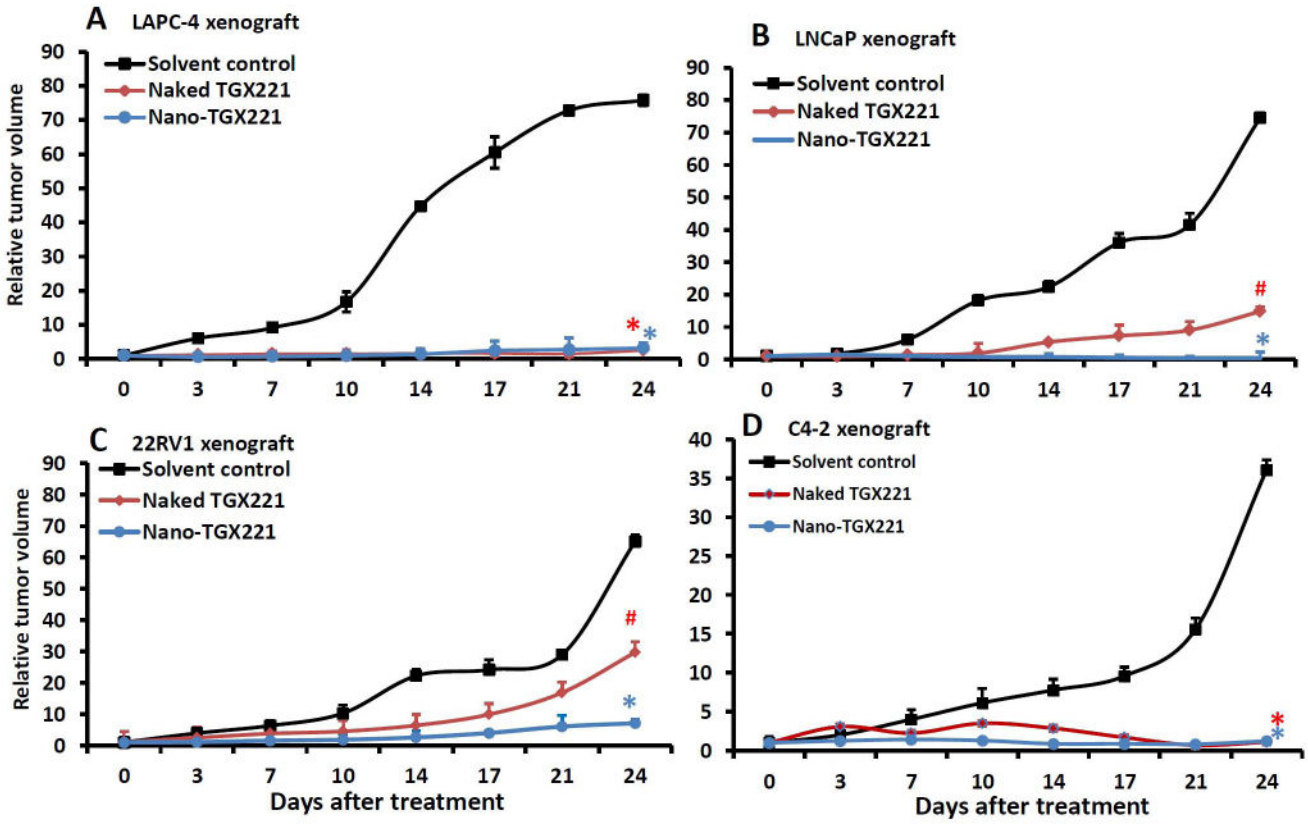

Fig 2.

Systemic delivery of TGX221 suppresses xenograft tumor growth derived from prostate cancer cells in nude mice. Xenografts were established from prostate cancer LAPC-4 (**A**), LNCaP (**B**), 22RV1 (**C**) and C4-2 (**D**) cells. Once xenograft tumors were palpable, animals were randomized into three groups (n = 8) and treated with intravenous injection of the PPG solution (solvent control), TGX221-BL05 dissolved in PPG (naked TGX221) or nanomicellar TGX221-BL05 (nano-TGX221). Drugs were used at a dose of 100 mg/Kg body weight in 200 μl volume *via* tail vein twice a week for 3 weeks. Tumor sizes were monitored at each treatment and presented as a percentage value at the measurement compared to the size on the first day of treatment. Data were presented as the Mean and error bars indicate the SEM. The asterisk and pone signs indicate significant differences compared to the control group (ANOVA analysis, * $P < 0.01$, # $P < 0.05$).

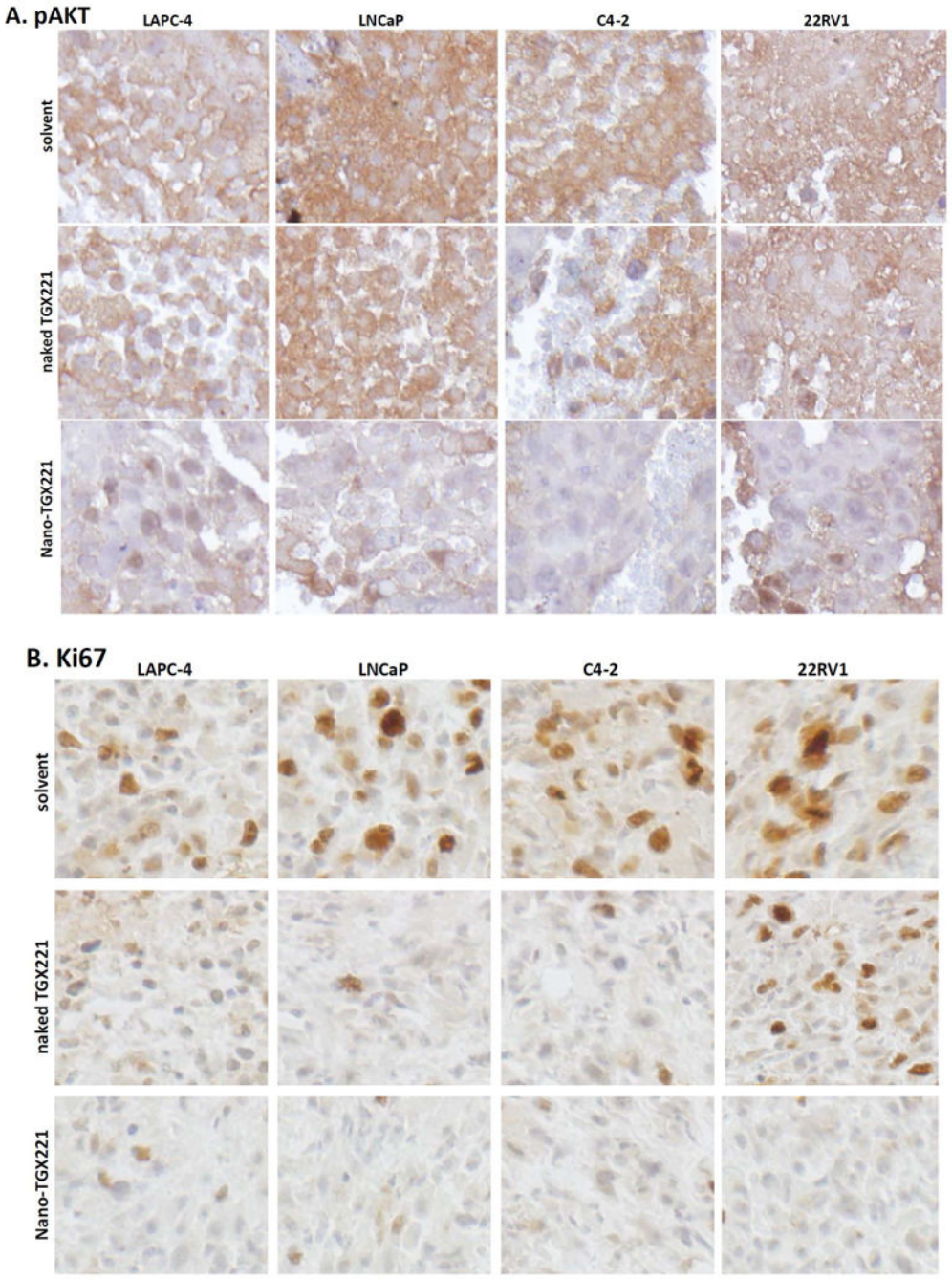

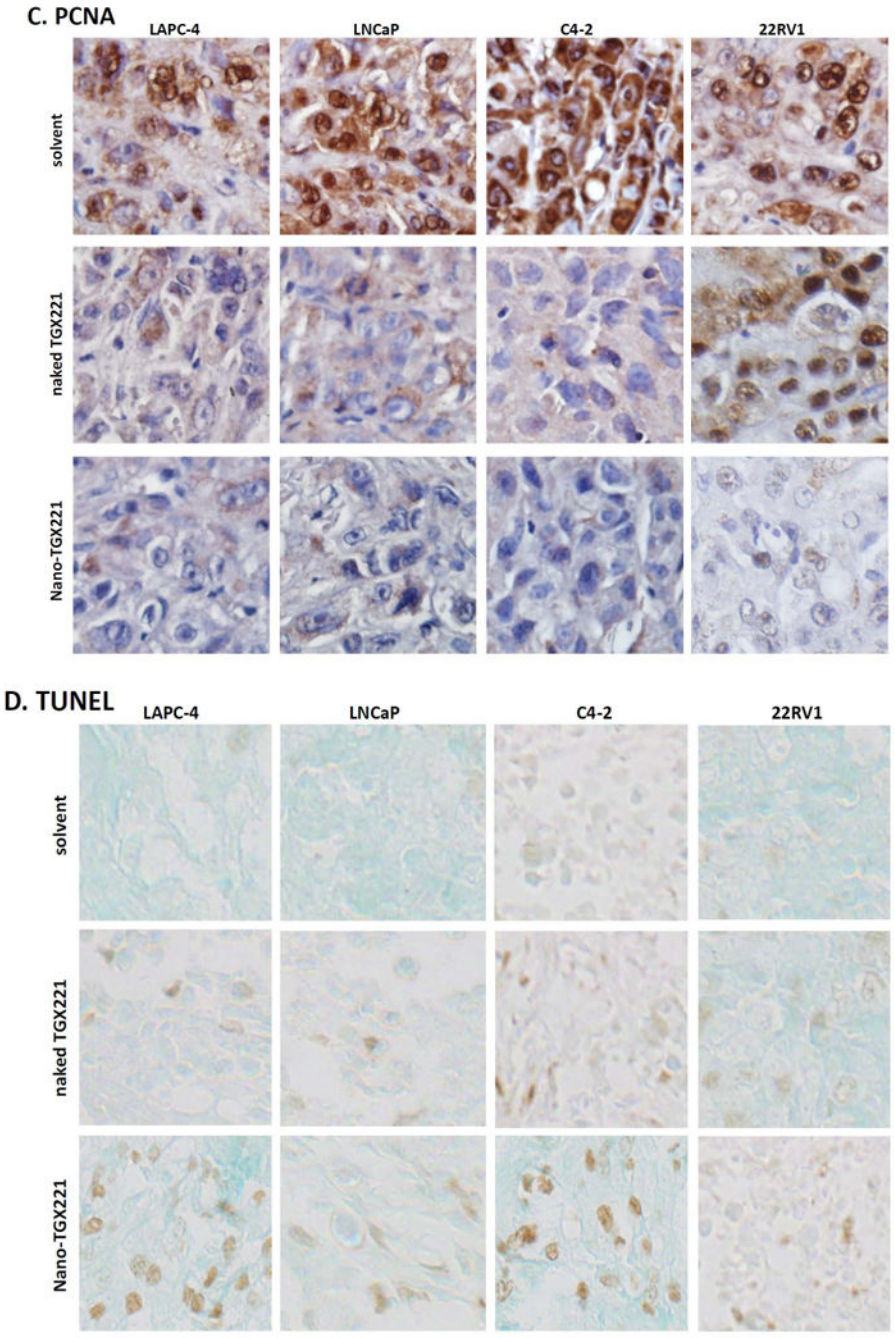

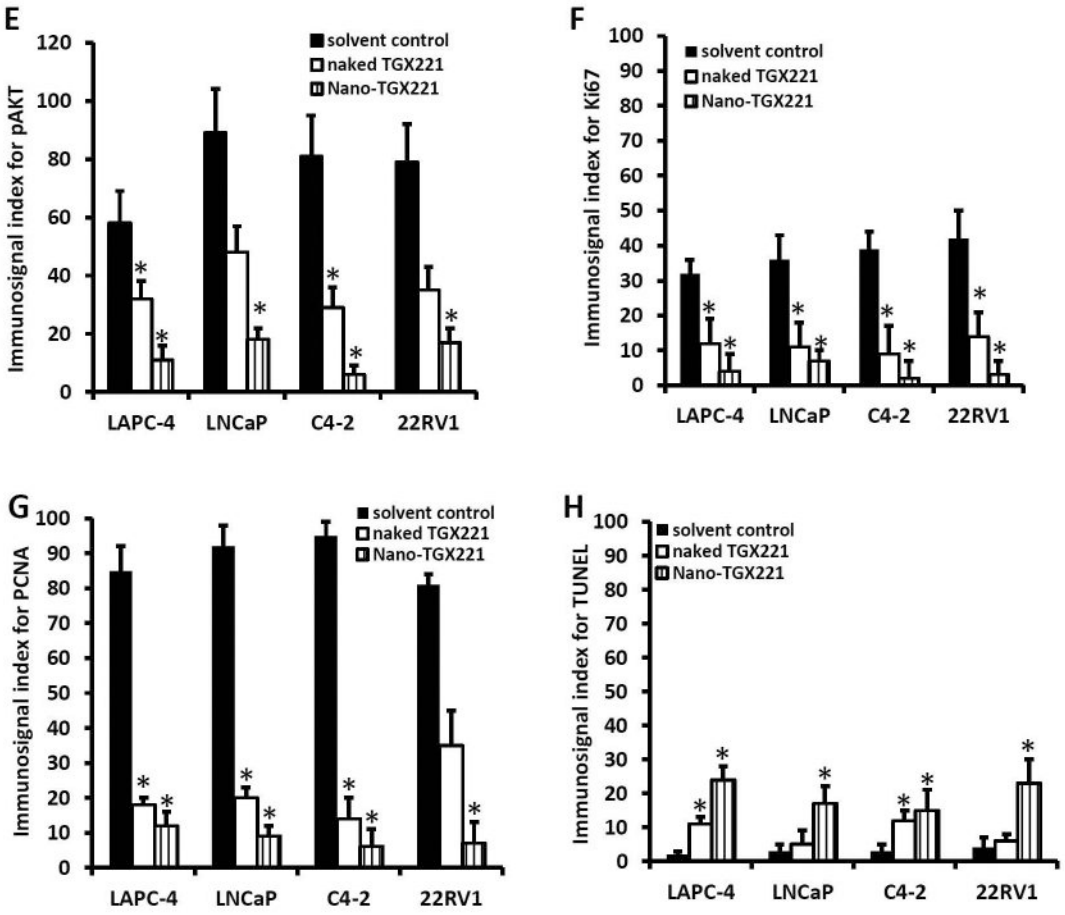

Fig 3.

A-D TGX221 suppresses AKT phosphorylation (**A**), reduces cell proliferation (**B**, Ki67; **C**, PCNA) and induces apoptosis (**D**, TUNEL). Paraffin-embedded tissue sections from harvested xenografts after treatment indicated on the left side of the panel (as described in Fig 2) were used for the immunostaining with antibodies listed on each panels. Representative microscopic images were shown for the immunostaining results. Magnification, × 200.

E-H Quantitative data from each immunostaining assays were summarized as average value (MEAN) of the immnosignal indexes as described (24). Error bars indicate the SEM of the MEAN. The asterisks indicate significant differences compared to the solvent control ($P < 0.05$, Student *t*-test).

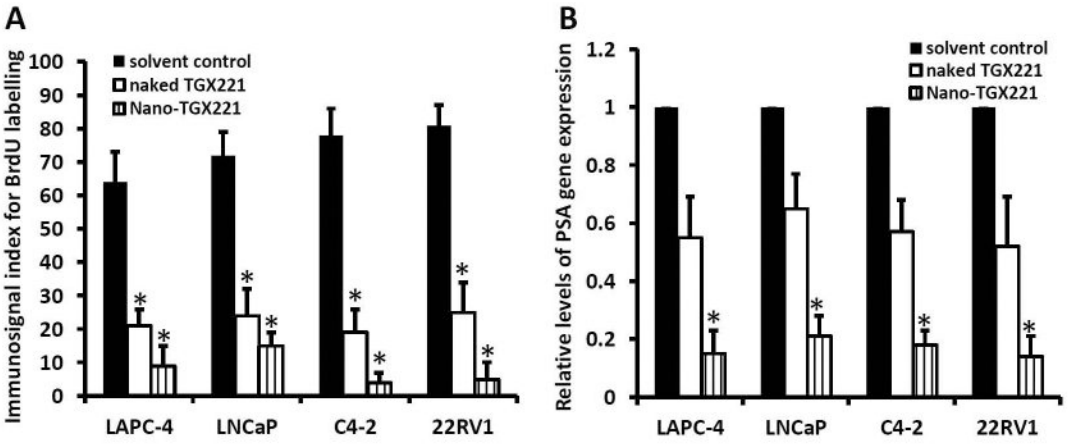

Fig 4.

TGX221 treatment reduces cellular BrdU labeling (**A**) and *PSA* gene expression (**B**) in prostate cancer xenograft tumors in nude mice.

A BrdU labeling assay was conducted at the end of drug treatment with intraperitoneal injection of 100 μl BrdU solution as described in our previous publication (24). After tissue harvesting, paraffin-embedded sections were used for anti-BrdU immunostaining and the average (MEAN) of the quantitated immunosignals indexes as described (24) were shown in each xenograft tumor group.

B Total RNA samples were extracted form tissue specimens of xenograft tumors harvested from animals after drug treatment. Quantitative RT-PCR assays were conducted to examine PSA gene expression at the mRNA levels and the relative levels of PSA gene expression from each group (n = 8) were presented as the MEAN. Error bars represent the SEM of the MEAN and the asterisk indicates a significant difference compared to the Solvent control (Student *t*-test, $P < 0.05$).